Fibers and Polymers 2005, Vol.6, No.2, 95-102

Preparation of Regenerated Cellulose Fiber via Carbonation (II) – Spinning and Characterization –

Sang Youn Oh, Dong Il Yoo*, Younsook Shin[1], Hak Yong Kim[2], Hwan Chul Kim[2], Yong Sik Chung[2], Won Ho Park[3], and Ji Ho Youk[4]

Department of Textile Engineering, Chonnam National University, Gwangju 500-757, Korea
[1]Department of Clothing & Textiles, Chonnam National University, Gwangju 500-757, Korea
[2]Department of Textile Engineering, Chonbuk National University, Jeonju 561-756, Korea
[3]Department of Textile Engineering, Chungnam National University, Daejeon 305-764, Korea
[4]Department of Textile Engineering, Inha University, Incheon 402-751, Korea
(Received June 9, 2004; Revised March 9, 2005; Accepted March 16, 2005)

Abstract: Sodium cellulose carbonate (CC-Na) dissolved in 8.5 wt% NaOH/ZnO (100/2-3, w/w) aqueous solution was spun into some acidic coagulant systems. Diameter of regenerated cellulose fibers obtained was in the range of 15-50 μm. Serrated or circular cross sectional views were obtained by controlling salt concentration or acidity in the acid/salt/water coagulant systems. Velocity ratio of take-up to spinning was controlled up to 4/1 with increasing spinning velocity from 5 to 40 m/min. Skin structure of was developed at lower acidity or higher concentration of coagulants. Fineness, tenacity and elongation of the regenerated cellulose fibers were in the range of 1.5-27 denier, 1.2-2.2 g/d, and 8-11.3 %, respectively. All of CC-Na and cellulose fibers spun from CC-Na exhibited cellulose II crystalline structure. Crystallinity index was increased with increasing take-up speed.

Keywords: Sodium cellulose carbonate (CC-Na), Regenerated cellulose fiber, NaOH/ZnO solution, Wet spinning, Tensile property, Crystalline structure

Introduction

Cellulose, the most abundant polysaccharide on the earth, has been used in many industrial fields [1,2]. Changing the shape by melt or dissolution is very important for the industrial applications. However, cellulose is insoluble in most of solvents and also does not melt until thermal degradation because of intra- and inter-molecular hydrogen bonding. To dissolve cellulose, the solvent molecules can be diffused into cellulose molecules and disrupt the crystallites [3]. Fiber industry is the most important among the application fields of cellulose. As direct solvent systems, two processes were developed as the cupro process using cuprammonium hydroxide solution and the lyocel process from monohydrate of N-methyl-N-morpholine oxide [4-6].

The intrinsic insolubility of cellulose in many solvent systems has provided considerable stimulus to prepare chemically modified cellulose. Typically, viscose rayon is manufactured by xanthation of alkali cellulose and the regeneration to cellulose during spinning step. Many processes were introduced to improve the viscose process, basic chemistry generating hydrogen sulfide and other by-products in spinning step causes environmental pollution [7,8]. The lyocel process developed recently is the most successful example among regenerated cellulose fibers manufactured by eco-friendly manner. Still many attempts are made such as breakdown of hydrogen bonding by steam explosion or carbamation made cellulose soluble in an aqueous sodium hydroxide solution [9-12]. Our research is an another attempt to get regenerated cellulose fiber by introducing carbonation reaction to alkali cellulose for the dissolution in an aqueous sodium hydroxide solution [13]. By the reaction of alkali cellulose and carbon dioxide, we introduced the cellulose carbonate and confirmed it by FT-IR [14].

In this study, we obtained regenerated cellulose fibers by spinning the dope solutions of carbonated cellulose into some acidic coagulant systems. And their cross-sectional and internal structures, mechanical and structural properties were also characterized.

Experimental

Materials

Pulp sheet (Cellunier-F, Rayonier Fernandina Mill, DP 850) was shredded to powders (ϕ1 mm), which has ca. 92 % of α-cellulose content. Commercially available compressed CO_2 gas was used and other reagents for CO_2 treatment. All the chemicals for dissolution, and spinning were used as purchased.

Carbonation of Cellulose

Alkali cellulose was prepared by steeping shredded cellulose pulp in 17.5 wt% NaOH solution at 25 °C for 2 h. After steeping, the alkali cellulose was filtered, neutralized to get alkali-treated cellulose with excess water, and then dried at 60 °C. Sodium cellulose carbonate (CC-Na) was obtained by treating

*Corresponding author: diyoo@chonnam.ac.kr

alkali cellulose with CO_2/ethyl acetate (EA) at −5-0 °C and 40-50 bar of CO_2 for 2 h. After the reaction, CC-Na was filtered, washed, and oven dried at 60 °C.

Spinning and Regeneration

Spinning dope was prepared by dissolving 5-5.5 % of CC-Na in 8.5 wt% NaOH/ZnO(100/2-3, w/w) at 0 °C. The dope solution of CC-Na was filtered, de-aerated and then transferred to a reservoir of the spinning equipment. The spinning dope in the reservoir was fed by N_2 gas to the spinneret, made of tantalum. Diameter of the spinneret used was 0.1 mm (1-30 hole). Regenerated cellulose fibers were prepared by using the wet spinning method with acid/salt/water or acid/water coagulant. One-bath and two-bath system for wet-spinning and the coagulant systems introduced in this study are shown in Figure 1 and Table 1, respectively. Spinning velocities were in the range of 8-40 m/min in one-bath system and 5-20 m/min in two-bath system. The ratio of spinning to take-up to spinning velocities was in the range of 1/1-4/1 in the one-bath system and 1/1-2/1 in the two-bath system. The temperatures of first and second coagulation bath were also set at room temperature and 60 °C, respectively. The scheme of carbonation and spinning is briefly shown in Figure 2.

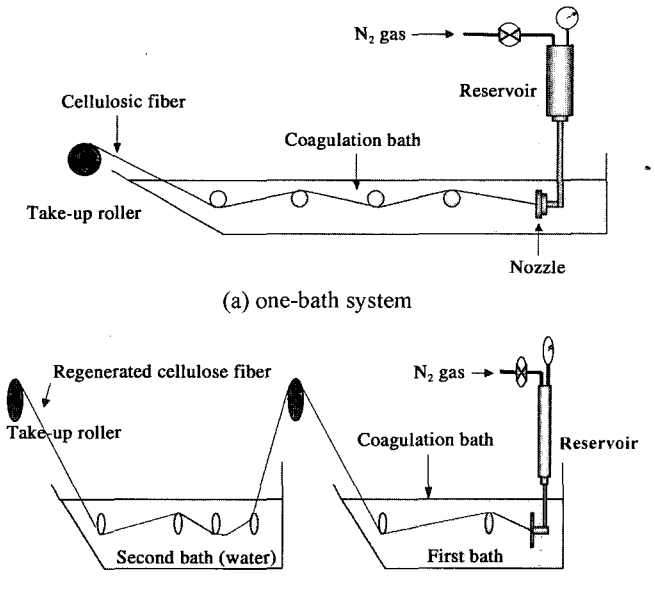

Figure 1. Schematic diagram of spinning apparatus.

Table 1. Coagulants used in this study

Coagulants	Weight ratio (w/w)
$H_2SO_4/Na_2SO_4/H_2O$	1/2/7
$CH_3COOH/CH_3COONa/H_2O$	1/1/1.8
CH_3COOH/H_2O	1/1.8
H_3PO_4/H_2O	1/3
H_2SO_4/H_2O	1/7

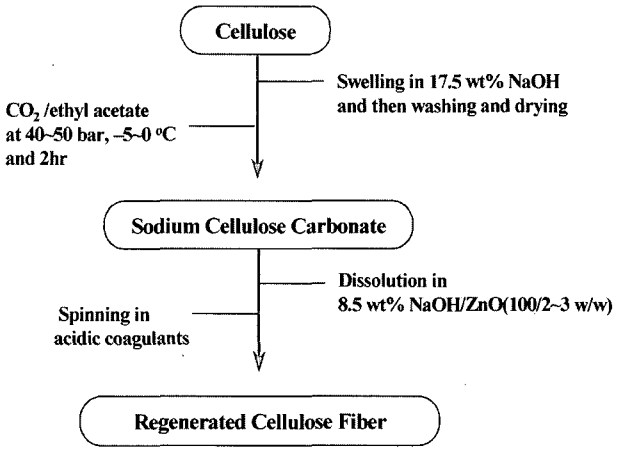

Figure 2. Carbonation and spinning process in this study.

Solubility and Phase Diagram of Cellulose Carbonate

The solubility of CC-Na was evaluated by observing transparency of cellulose solution using optical microscope (OPHIPHOT-POL, Nikon, Japan) at the magnification of 200. Absorbance indicating turbidity of cellulose solutions was measured by using UV-Vis spectrophotometer (Shimadzu UV-2101PC, Japan). The solubility of CC-Na dissolved in 8.5 wt% NaOH/ZnO (100/0-3, w/w) was evaluated and then phase diagram of CC-Na was obtained with the change of its concentration and ZnO concentration in aqueous NaOH solution.

Microscopic Observation of Fiber Cross-Section

Cross-sectional diameters and shapes of regenerated cellulose fibers were obtained by using a scanning electron microscope (JEOL JSM-5400) and an optical light microscope (OPHIPHOT-POL, Nikon). A bundle of regenerated fibers was attached to a conductive double-sided stick tape and cut close to the side of the tape. The tape was attached to a sample stub and coated with 20-30 nm Au-Pd alloy prior to being imaged at 5-20 kV. In order to observe the skin-core structure, cellulose fibers were dyed in advance by methyl violet at 40 °C for 40 min. The liquor ratio of 100/1 and the concentration of 0.015 % (o.w.f.) were used. The dyed fibers were washed with distilled water three times and ethyl alcohol, and then dried at 60 °C. Cross-sectional views of the dyed fibers were observed with an optical light microscope (LABORLUX-12-POL, Leitz, Germany) at the magnification of 250.

Tensile Property Measurement

The tensile test was performed according to KSK 0323 (C.R.E. single strand method) by using universal testing machine (United Calibration Corporation, STM-5). The length between clamps and elongation rate were 20 mm and 20 mm/min, respectively. Wet tenacity and elongation of fiber steeped in distilled water at 20 ± 2 °C for 3 min were measured.

X-ray Diffraction Analysis

Crystalline structures of cellulose, alkali cellulose, CC-Na, and regenerated cellulose fibers were analyzed by wide angle X-ray diffractometer (Rigaku-D/MAX Uitima III, Japan) with 5 °/min scan speed. The cellulose powder was laid on the glass sample holder (35 × 50 × 5 mm) and analyzed at plateau condition. Ni-filtered Cu-Kα radiation (λ = 1.54 Å) generated at a voltage of 40 kV and current of 40 mA was utilized and the scan speed of 2 °/min from 5 ° to 50 °. The crystalline index (CI) was calculated by

$$CI = 1 - h_{am}/h_{cr} = 1 - h_{am}/(h_{tot} - h_{am})$$

where h_{cr} is crystalline height at 2θ of 19.8 ° and h_{am} is the height of amorphous reflection at 2θ of 16 ° [15]. For the curve fitting, Lorentzian function was selected during the operation of Microcal™ Origin™ (Microcal software Inc.). And also the amorphous halos were drawn for the determination of h_{am}.

Results and Discussion

Solubility and Phase Diagram

Several solubility test methods such as optical microscopic observation, DSC experiment and centrifuge were used in other papers for cellulose. Optical microscopic observation was used in cellulose/NMMO solution for obtaining phase diagram consisted of different contents of H_2O and cellulose in NMMO solution [16,17]. Olga Biganska and Patrick Navard showed the full phase diagram of NMMO-water mixture by DSC experiment. It was built from DSC experiments of many NMMO-water compositions with several calorimeters in two different locations [18].

In our study, solubility was evaluated by observing the turbidity of solution using optical microscope and absorbance by UV-Vis spectrophotometer. Optical microphotographs of cellulose solutions with different solubility were reported [13]. Solubility was divided into three such as soluble (●), soluble incompletely (▲) and gel (○). In UV-Vis spectra, absorbance at 400 nm was clearly distinguishable between low and high solubility. So it was adopted for criterion of solubility evaluation [13]. According to the combining results of these solubility tests, phase diagram of cellulose were figured.

Figure 3 shows phase diagram of CC-Na in 8.5 wt% NaOH/ZnO system at 0 °C. The CC-Na concentration for initial gelation was decreased with decreasing zinc oxide content in aqueous sodium hydroxide solution. When zinc oxide content increased up to 3 wt%, the gelation was appeared at higher than 5.5 wt% of CC-Na concentration. Maximum concentration of cellulose carbonate for soluble zone was increased with increasing zinc oxide concentration. The solubility of cellulose samples in aqueous NaOH solution could be significantly enhanced by adding zinc oxide or urea to the system and/or by lowering the temperature of the treatment [19,20]. For

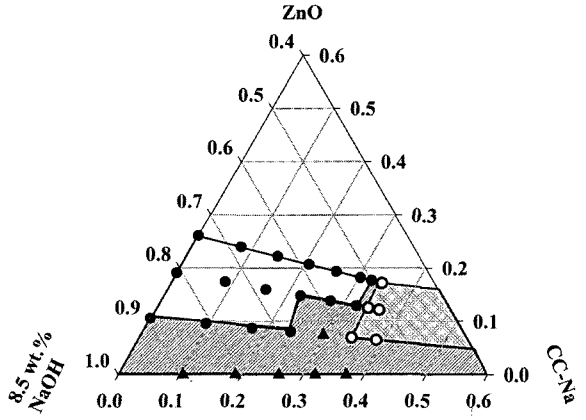

Figure 3. Phase diagram of CC-Na (●) soluble, (▲) soluble incompletely, (○) gel. Unit; CC-Na(or ZnO or NaOH) wt% / (CC-Na + ZnO + NaOH), wt%.

example, it was reported that the presence of zinc oxide led to an in-situ formation of zincate complex with facilitate the dissolution of cellulose chains such as short-chain up to the DP of about 200, even at room temperature [21]. These results indicate that the factors, affecting solubility of cellulose were concentration of it and zinc oxide content in NaOH solution.

Cellulose chains generally interact with each other through hydrogen bonding and van der Waals forces to form extensive crystalline regions. These inter-chain hydrogen bonds in the crystalline regions present a formidable barrier against the penetration by reagents, so cellulose is insoluble in most liquids such as water and polar organics. In our NaOH/ZnO system, zinc acid anions created by reacting zinc oxide with aqueous sodium hydroxide solution are expected to diffuse into cellulose chains and destruct hydrogen bonding through carbonation process and ion-dipole interaction between zinc acid anions and cellulose hydroxyl groups.

At certain concentration of cellulose in dissolving procedure, gelation is occurred due to the aggregation of cellulose chains. These aggregates, that were consisted of highly ordered cylindrical core of aligned chains with two spherical coronas surrounding core ends which had an effect on cellulose solubility, were reported [22]. In our study, the boundary between soluble and gel of cellulose solution was very narrow and phase of cellulose solution was changed into gel fast with increasing cellulose concentration.

Spinning and Regeneration

As reported in previous paper, sodium cellulose carbonate (CC-Na) was prepared by the reaction of alkali cellulose and carbon dioxide gas and its solubility in aqueous sodium hydroxide solution was evaluated [13]. Based on liquid phase of carbon dioxide, carbonation condition selected was were −5-0 °C and 40-50 bar. Whole range of CC-Na concentration prepared in sodium hydroxide solution was evaluated by the criterion of solubility. The solubility of CC-Na in sodium

hydroxide solution only was not sufficient as a dope solution, because carbonation was taken place in smaller amorphous region. Presence of zinc oxide plays a role to form zincate complex in sodium hydroxide solution facilitates the dissolution of cellulose chains up to the degree of polymerization of about 200 [23]. Confirming this in a preliminary experiment, we selected 8.5 wt% aqueous NaOH/ZnO (100/2-3 wt%) as a dope medium. Because of the restricted solubility of ZnO, it was dissolved in concentrated aqueous NaOH about 50 wt% and then diluted with water up to 8.5 wt% NaOH solution.

As same as viscose process, we employed acidic coagulant systems for the regeneration of cellulose. Because the regeneration of cellulose is very complex, chemical and physical transformation is not easy to characterize. In viscose process, 1-4 wt% $ZnSO_4$ was added to coagulant bath for making transient zinc-cellulose xanthate complex. This transient zinc complex was believed to responsible for the formation of large skin structure which gave greater crystallinity by delaying regeneration relative to sodium cellulose xanthate (the zinc variant is more stable), and possibly also by cross-linking between neighbouring cellulose chains, allowing greater orientation to be achieved [24].

Fiber formation in wet spinning is controlled by diffusion processes so that spinning velocities are controlled not higher than 50-150 m/min. The slower build-up of the fiber texture is important to control the regeneration process and also to get better fiber properties. We introduced varieties of coagulant, bath system such as one- or two- bath, and ratio of spinning to take-up velocities to obtain the optimum condition of regeneration and orientation. For both coagulation bath systems, the velocity ratio of take-up to spinning was controlled with increasing spinning velocity from 5 to 40 m/min. By setting the temperatures of first and second bath differently, it was possible to control the regeneration and stretching in two-bath system more effectively. Because fiber spun through the two-bath system is imposed more load than the one-bath system, the ratio of take-up to spinning velocities of two-bath system (1/1-2/1) was lower than that of one- bath system (1/1-4/1).

Cross-Sectional View and Skin-Core Structure

Figure 4 shows cross-sectional SEM images of cellulose fibers prepared with some coagulants listed in Table 1. Diameters of cellulose fibers spun were in the range of 15-50 μm, which is a little bit larger that those of conventional cellulose fibers (10-20 μm) [25]. They showed different cross-sectional shapes according to the type of coagulant. The spinnability of CC-Na solution was tested for five coagulants at some compositions and derived optimal compositions of given coagulants. As same as the viscose process, we obtained the serrated view by using salt in the coagulants in Figure 4. Thick skin structures of cellulose fibers are induced in the presence of salt coagulants. But the serrated shapes of cellulose fibers were less developed than that of regular viscose rayon.

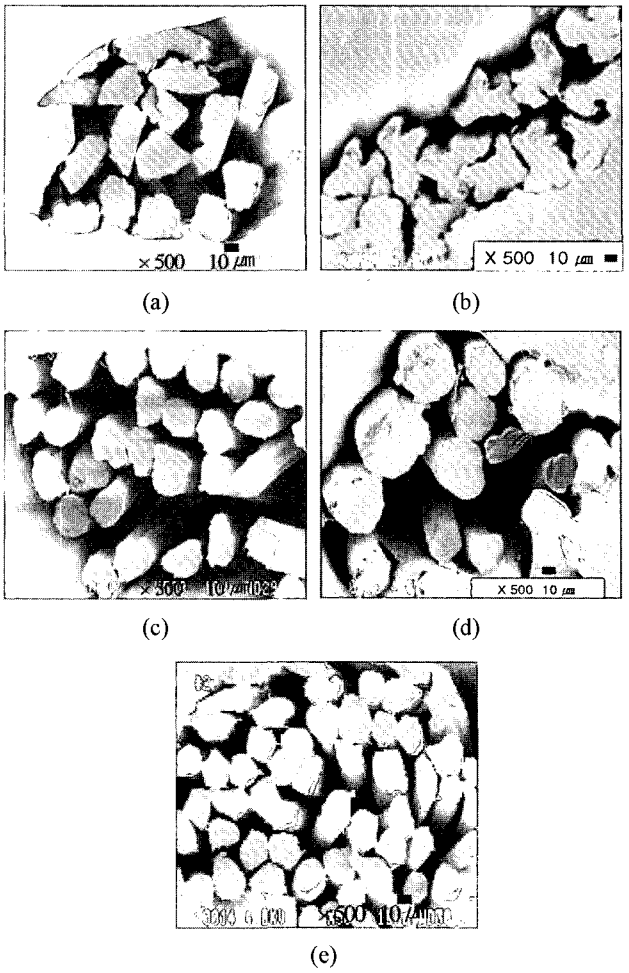

Figure 4. SEM images of regenerated cellulose fibers (scale bar 10 μm) prepared at some coagulation systems: (a) $H_2SO_4/Na_2SO_4/H_2O$, (b) $CH_3COOH/CH_3COONa/H_2O$, (c) CH_3COOH/H_2O, (d) H_3PO_4/H_2O, and (e) H_2SO_4/H_2O.

It is regarded that zincate complexes contributes to the stability of dope solution but has slower diffusion rate than sodium hydroxide hydrates.

Since natural celluloses is of high crystallinity, hydroxyl groups in small amorphous region are available for dyeing with basic dyes [26]. When regenerated cellulose fibers are dyed with basic dyes such as diphenyl methane and diphenyl naphthyl methane, we can differentiate skin and core region from the cross-sectional view [27]. We dyed the regenerated cellulose fibers by methyl violet followed by washing with distilled water and ethyl alcohol. In the case of acid/salt/water coagulants, cellulose fibers showed the skin-core structure as shown in Figure 5. The skin region of cellulose fiber spun in $CH_3COOH/CH_3COONa/H_2O$ was larger than that spun in $H_2SO_4/Na_2SO_4/H_2O$. This is in good agreement that the skin region of cellulose fiber spun into low acidity coagulant was larger than that spun into high acidity coagulant [26]. The difference by acidity of coagulant is shown well in viscose

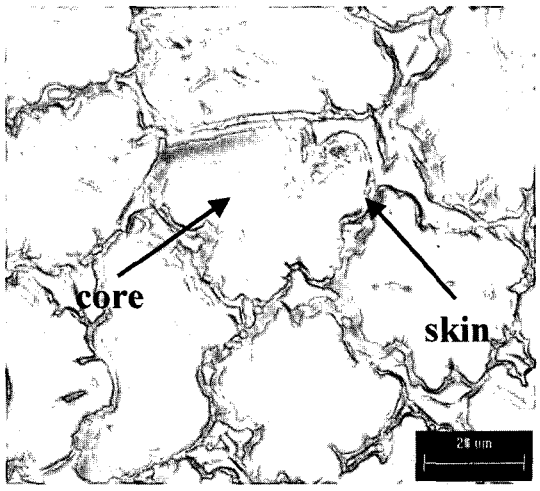

(a)

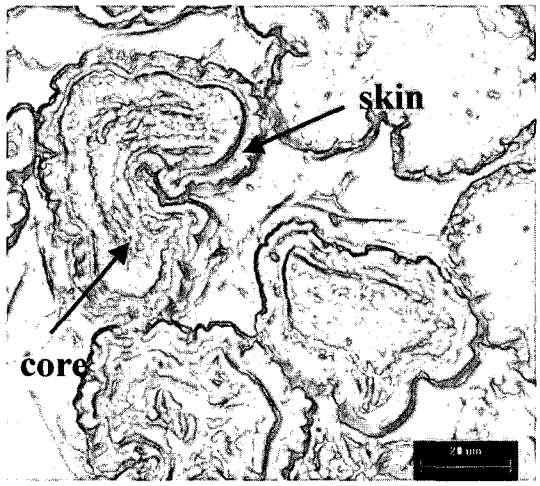

(b)

Figure 5. Cross-sections of dyed regenerated cellulose fibers prepared at the coagulation systems of (a) $H_2SO_4/Na_2SO_4/H_2O$ and (b) $CH_3COOH/CH_3COONa/H_2O$.

rayon (thin skin) and polynosic (all skin). In the case of coagulants consisted with acid/water such as the skin structure was not developed well. It is also understood from the fact that the regeneration of fiber spun into the bath without salt is more rapid than that with salt [26].

Tensile Properties

Regenerated cellulose fibers of diverse structures lead to various properties and subsequent application fields. Fiber structure of the regenerated fiber structure can be controlled by introducing diverse manufacturing processes. Though typical fiber fineness would be in the range 0.9-4.5 denier (10-20 μm in diameter), it is available up to around 45 denier (60 μm) [25]. Cross sectional areas of the regenerated fibers were calculated from the contour of microscopic view. From the diameters measured of about 12-50 μm, fineness of regenerated cellulose

Table 2. Tenacity and elongation of regenerated cellulose fibers at different bath system

		Coagulant condition (weight ratio)		
		$H_2O:H_2SO_4:Na_2SO_4:ZnSO_4$, 7:1:1.25:0.5 (Two-bath)	$H_2O:H_2SO_4$, 7:1.5 (Two-bath)	$H_2O:H_2SO_4$, 7:1.5 (One-bath)
Average diameter (μm)		17	19	14
Fineness (denier)		2.92	3.64	1.98
Tenacity at break (g/d)	Dry	1.36	1.96	2.23
	Wet	1.17	2.58	1.67
	Wet/Dry	0.86	1.32	0.75
Elongation at break (%)	Dry	8.85	11.27	8.75
	Wet	14.32	13.23	9.58
	Wet/Dry	1.62	1.18	1.10

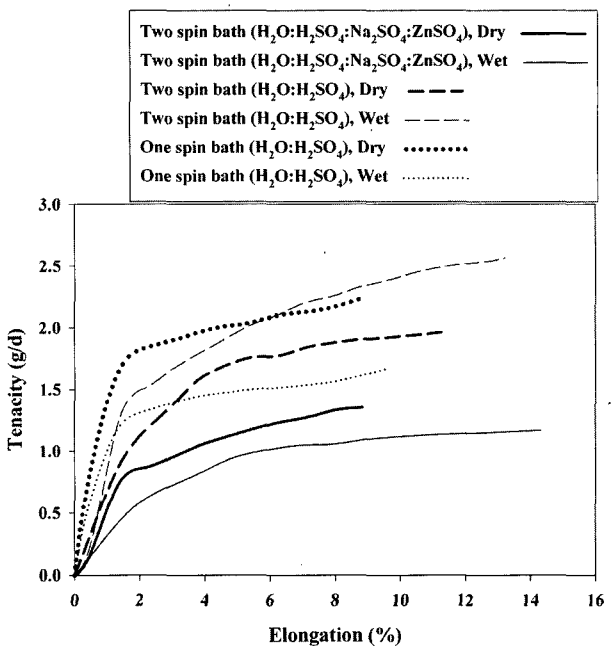

Figure 6. Tenacity-elongation curves of regenerated cellulose fiber at some coagulation systems.

fibers were calculated in the range of 1.5-27 denier. As the take-up velocity was increased at a constant spinning velocity or extruding velocity, the fineness was decreased.

Tensile properties obtained according to the KSK 0323 single strand method at various spinning bath systems and coagulation conditions are shown in Table 2. We introduced two-bath system with and without salt as a coagulant. And also we used the coagulant system of sulfuric acid only in one-bath system because it was difficult to remove remaining salt in the filament. Finer filament was obtained in one-bath (sulfuric acid coagulant) system. Tenacity and the ratio at wet/dry state of regenerated cellulose fibers in one-bath system

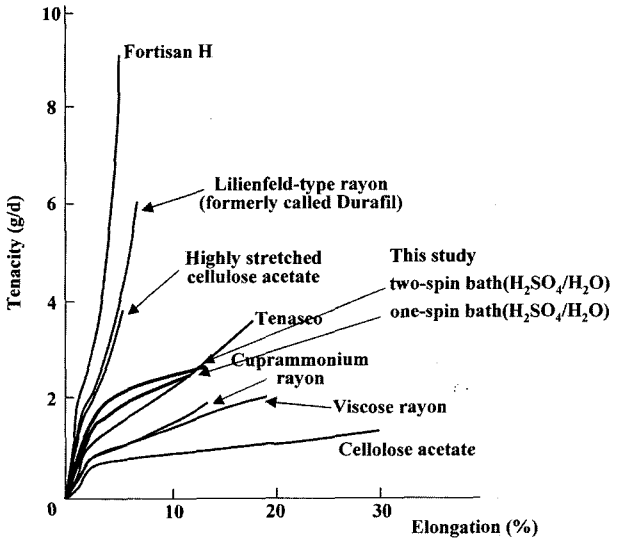

Figure 7. Tenacity-elongation curves of various regenerated cellulose fibers [24].

were higher than that by two-bath system. However, elongation and the ratio at wet/dry state of mixed salt system were higher than those of sulfuric acid system. Figure 6 shows tenacity-elongation curves at some coagulant systems. The systems without salt gave relatively higher tenacity but lower elongation than the system with salt.

The regenerated fibers obtained in this study showed lower tenacity and elongation than other cellulosic fibers except for cellulose acetate and viscose rayon (Figure 7). In spite of high molecular weight of cellulose used, tensile property is caused by the fact that the regenerated fibers had low crystallinity due to incomplete stretching or orientation, no heat treatment, and low content of $ZnSO_4$ in coagulants. In the viscose process, 1-4 wt% $ZnSO_4$ was added to coagulant bath to make transient zinc-cellulose xanthate complex. This transient zinc complex was responsible for the formation of large skin structure which gave higher crystallinity by delayed regeneration, and also for cross-linking between neighboring cellulose chains, allowing greater orientation [26]. However, the tenacity ratio for the wet spinning to the dry spinning was 0.75-1.32, which was higher than that of regular viscose rayon (*ca.* 0.5).

Crystalline Structure

Figure 8 shows X-ray diffraction curves of alkali-treated cellulose, CC-Na and the regenerated cellulose fiber from CC-Na. Diffraction angles (2θ) at 12.1 °, 19.8 °, and 22.0 ° are correspondent to monoclinic ($1\bar{1}0$), (110), and (200) planes, respectively. The curves of alkali-treated cellulose and CC-Na indicate clearly cellulose II structure. However, the peaks correspond to 19.8 ° and 22.0 ° of the regenerated cellulose fiber are overlapped and does not show well defined cellulose II structure.

Curve fitting was introduced for the analysis of X-ray

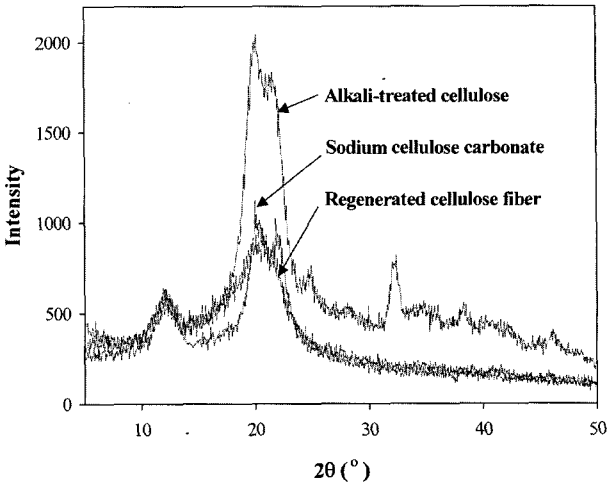

Figure 8. Wide angle X-ray diffraction curves of alkali-treated cellulose, CC-Na, and regenerated cellulose fibers from CC-Na.

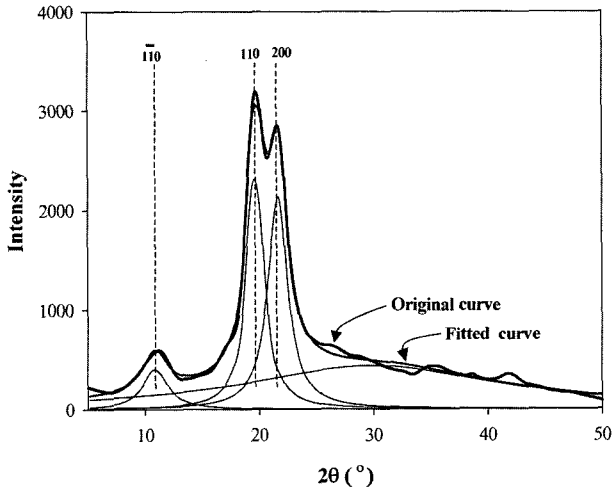

Figure 9. X-ray diffraction pattern of alkali-treated cellulose and Lorentzian curve deconvoluted (fitted curve is the sum of the other curves deconvoluted from the X-ray diffraction pattern).

diffraction pattern as shown in Figure 9. Consequently, the curve fitting of the alkali-treated cellulose, CC-Na and regenerated cellulose fiber revealed cellulose II structure. Cellulose II is prepared from cellulose samples with other crystal forms or with amorphous structures by regeneration or mercerization [28,29]. Cellulose II has a monoclinic unit cell consisting of two cellulose chains with a P21 space group. At right angles to the chain direction, the unit cell is a parallelogram with an angle of about 62 ° and sides of about 0.801 nm (a-axis), 0.904 nm (b-axis), 1.036 nm (c-axis) and 117 ° (γ) [30]. For the determination of crystallinity index (CI), Segal *et al* introduced the ratios between the crystalline scatter of the 002 reflection at 2θ of 22.5 ° in the case of cellulose I or 101 reflection at 2θ of 19.8 ° in the case of cellulose II (crystalline height, h_{cr}) and the height of the

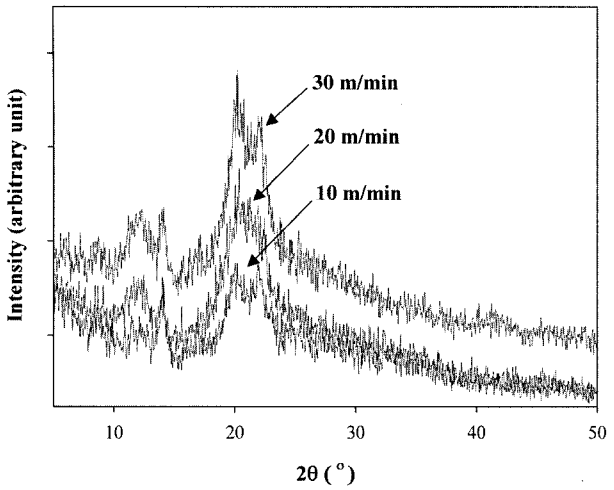

Figure 10. Wide angle X-ray diffraction curves of regenerated cellulose fiber spun into sulfuric acid/water system (one bath) at some take-up velocities (spinning speed 8 m/min).

"amorphous reflection" at 2θ of 18 ° for cellulose I or 16 ° for cellulose II (amorphous height, h_{am}), respectioely [22]. In this study, CI of the alkali-treated cellulose, CC-Na and regenerated cellulose fiber were calculated as 0.65, 0.49 and 0.42, respectively. CI of the CC-Na was considerably decreased compared with that of alkali-treated cellulose. This indicates that introduction of carbonated groups increases amorphous region and disrupts intra- or inter-molecular hydrogen bonding of cellulose, subsequently. Broader amorphous region of CC-Na strongly supports the indication.

Figure 10 shows X-ray diffraction patterns of regenerated cellulose fibers, which were spun into sulfuric acid/water system (one-bath) at some take-up velocities. With the help of curve fitting, CI of the fibers calculated at the take-up velocity of 10, 20 and 30 m/min were 0.15, 0.25 and 0.33, respectively. As anticipated, CI is increased with increasing take-up velocity.

Conclusions

Sodium cellulose carbonate dissolved in aqueous NaOH/ZnO solution were spun into some acidic coagulation baths. One- and two-bath systems were introduced to get regenerated cellulose fibers. Diameters of cellulose fibers obtained were in the range of 15-50 μm. Serrated or circular cross section of cellulose fibers was obtained by controlling salt concentration in coagulants of acid/salt/water system. Skin structure of cellulose fibers was developed by spinning into coagulants of low acidity or high concentration. Varieties of coagulants, bath systems such as one- or two- bath, and the ratio of spinning to take-up velocities were introduced to obtain an optimum condition of regeneration and orientation. Velocity ratio of take-up to spinning was controlled up to 4/1 with increasing spinning velocity from 5 to 40 m/min. Fineness, breaking tenacity and elongation of the filament in dry were 1.5-20 denier, 0.5-2.4 g/d, and 8-14 %, respectively. Both of sodium cellulose carbonate (CC-Na) and the regenerated cellulose fiber showed typical cellulose II structure. Crystallinity index calculated with the help of curve fitting was increased with increasing take-up speed.

Acknowledgements

This work was supported by grant No. (R01-2001-00522-0) from the Korea Science & Engineering Foundation.

References

1. N. Jinmin, Y. Fujita, T. Arai, A. Kondo, Y. Morikawa, H. Okada, M. Ueda, and A. Tanaka, *Journal of Molecular Catalysis B: Enzymatic,* **17**, 197 (2002).
2. J. Tkáç, I. Voštiar, P. Gemeiner, and E. Šturdík, *Bioelectrochemistry,* **55**, 149 (2002).
3. A. F. Turbak, R. B. Hammer, R. E. Davies, and H. L. Hergert, *Chemtech.*, **10**, 51 (1980).
4. H. P. Fink, P. Weigel, H. J. Purz, and J. Ganster, *Progress in Polymer Science,* **26**, 1473 (2001).
5. T. Rosenau, A. Potthast, H. Sixta, and P. Kosma, *Progress in Polymer Science,* **26**, 1763 (2001).
6. O. Biganska and P. Navard, *Polymer,* **44**, 1035 (2003).
7. R. W. Moncrieff, "Man-Made Fibres", 6th Ed., pp.162-299, Newnes-Butter Worths, London, 1975.
8. J. I. Kroschwitz, "Polymers: Fibers and Textiles, A Compendium", pp.746-772, John Wiley & Sons, Inc., New York, 1990.
9. M. J. Negro, P. Manzanares, J. M. Oliva, I. Ballesteros, and M. Ballesteros, *Biomass and Bioenergy,* **25**, 301 (2003).
10. T. Jeoh and F. A. Agblevor, *Biomass and Bioenergy,* **21**, 109 (2001).
11. W. Mormann and U. Michel, *Carbohydrate Polymers,* **50**, 201 (2002).
12. A. M. A. Nada, S. Kamel, and M. E. Sakhawy, *Polymer Degradation and Stability,* **70**, 347 (2000).
13. S. Y. Oh, D. I. Yoo, Y. Shin, W. S. Lee, and S. M. Jo, *Fibers and Polymers*, **3**, 1 (2002).
14. S. Y. Oh, D. I. Yoo, Y. Shin, and G. Seo, *Carbohydrate Research*, **340**, 417 (2005).
15. H. A. Krässig, "Cellulose; Structure, Accessibility and Reactivity, Polymer Monographs V11", pp.88-90, Gordon and Breach Science Publishers, Switzerland, 1993.
16. N. E. Franks and J. K. Varga, *U.S. Patent*, 4,196,282, (1980).
17. A. F. Turbak, R. B. Hammer, R. E. Davies, and H. L. Hergert, *Chem. Technol.*, **11**, 702 (1977).
18. O. Biganska and P. Navard, *Polymer*, **44**, 1035 (2003).
19. G. F. Davidson, *J. Text. Inst.*, **28**, 27 (1937).
20. Z. Jinping and Z. Lina, *Polymer J.*, **32**, 866 (2000).

21. C. Bergner and B. Phillip, *Cellulose Chem. Technol.*, **20**, 591 (1986).
22. B. Morgenstern and H. W. Kammer, *Polymer J.*, **40**, 1299 (1999).
23. C. Bergner and B. Phillip, *Cellulose Chem. Technol.*, **20**, 591 (1986).
24. E. E. Treiber in "Cellulose and Its Derivatives", (T. P. Nevell and S. H. Zeronian Eds.), pp.454-469, Ellis Horwood Limited, Chiche, 1987.
25. J. W. S. Hearle in "Regenerated Cellulose Fibers", (C. Woodings Eds.), pp.201-202, Woodhead Publishing Limited, Cambridge, 2001.
26. R. W. Moncrieff, "Man-Made Fibres", 6th Ed., Newnes-Butter Worths, London, pp.164-168 and 279-289, 1975.
27. N. S. Wooding in "Rayon and Acetate Fibers", (J. W. S. Hearle and R. H. Peters Eds.), pp.41-57, in Fiber Structure, The Textile Institute, Manchester, 1963.
28. D. Gagnaire, D. Mancier, and D. M. Vincendon, *J. Polym. Sci., Polym. Chem. Edn.*, **18**, 13 (1980).
29. A. Sarko, J. Southwick, and J. Hayashi, *Macromolecules*, **9**, 857 (1976).
30. L. M. J. Kroon-Batenburg, J. Kroon, and M. G. Northolt, *Polym. Commun.*, **27**, 290 (1986).